

IN THE UNITED STATES PATENT AND TRADEMARK OFFICE

In re Application of:	Michael R. Rosen, <i>et al.</i>	Confirmation No.:	5518
Application No.:	10/757,827	Examiner:	A. K. Singh
Filed:	01/15/2004	Group Art Unit:	1632

For: ***Mesenchymal stem cells as a vehicle for ion channel transfer in syncytial structures***

Commissioner for Patents
Alexandria, VA 22313-1450

AFFIDAVIT UNDER 37 C.F.R. § 1.132

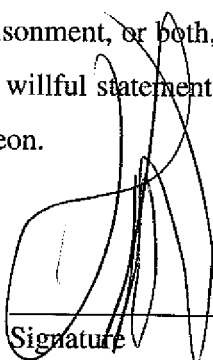
Dear Sir:

I, Michael R. Rosen, hereby attest to the following:

1. I am the Pfeiffer Professor of Pharmacology and Pediatrics; Director, Center for Molecular Therapeutics, Presbyterian Hospital, Room 7 W 321, 622 West 168th St., New York, NY 1003.
2. I am the co-inventor of the inventions disclosed in the above-identified application: Rosen et al., US Patent Application 10/757,827, filed on 1/15/2004, which claims priority to U.S. Provisional Application Ser. No. 60/440,265 filed on Jan. 15, 2003.
3. I am also co-inventor of the inventions disclosed in US Patent Application 09/875,388, 200201879481 filed on 6/6/2001, and in WO 02/098286, entitled Implantation of Biological Pacemaker that is Molecularly Determined, dated 12/12/2001.
4. I hereby declare that any invention disclosed but not claimed in Rosen, et al., US Patent Application 09/875,388 and in WO 02/098286, was derived from me and is thus not an invention "by another" with respect to Rosen et al., US Patent Application 10/757,827.

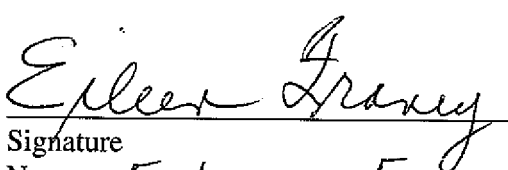
5. I hereby declare that all statements made herein of my own knowledge are true and that all statements made on information and belief are believed to be true; and further that these statements were made with the knowledge that willful false statements and the like so made are punishable by fine or imprisonment, or both, under Section 1001 of Title 18 of the United States code and that such willful statements may jeopardize the validity of the application or any patent issued thereon.

12-1-10
Date


Signature
Michael R. Rosen

Witnessed by:

12/1/10
Date


Signature
Name: Eileen Franey

Integrative Physiology

Human Mesenchymal Stem Cells as a Gene Delivery System to Create Cardiac Pacemakers

Irina Potapova,* Alexei Plotnikov,* Zhongju Lu, Peter Danilo, Jr, Virginijus Valiunas, Jihong Qu, Sergey Doronin, Joan Zuckerman, Iryna N. Shlapakova, Junyuan Gao, Zongming Pan, Alan J. Herron, Richard B. Robinson, Peter R. Brink, Michael R. Rosen, Ira S. Cohen

Abstract—We tested the ability of human mesenchymal stem cells (hMSCs) to deliver a biological pacemaker to the heart. hMSCs transfected with a cardiac pacemaker gene, mHCN2, by electroporation expressed high levels of Cs^+ -sensitive current (31.1 ± 3.8 pA/pF at -150 mV) activating in the diastolic potential range with reversal potential of -37.5 ± 1.0 mV, confirming the expressed current as I_f -like. The expressed current responded to isoproterenol with an 11-mV positive shift in activation. Acetylcholine had no direct effect, but in the presence of isoproterenol, shifted activation 15 mV negative. Transfected hMSCs influenced beating rate in vitro when plated onto a localized region of a coverslip and overlaid with neonatal rat ventricular myocytes. The coculture beating rate was 93 ± 16 bpm when hMSCs were transfected with control plasmid (expressing only EGFP) and 161 ± 4 bpm when hMSCs were expressing both EGFP+mHCN2 ($P < 0.05$). We next injected 10^6 hMSCs transfected with either control plasmid or mHCN2 gene construct subepicardially in the canine left ventricular wall in situ. During sinus arrest, all control (EGFP) hearts had spontaneous rhythms (45 ± 1 bpm, 2 of right-sided origin and 2 of left). In the EGFP+mHCN2 group, 5 of 6 animals developed spontaneous rhythms of left-sided origin (rate = 61 ± 5 bpm; $P < 0.05$). Moreover, immunostaining of the injected regions demonstrated the presence of hMSCs forming gap junctions with adjacent myocytes. These findings demonstrate that genetically modified hMSCs can express functional HCN2 channels in vitro and in vivo, mimicking overexpression of HCN2 genes in cardiac myocytes, and represent a novel delivery system for pacemaker genes into the heart or other electrical synchia. (*Circ Res.* 2004;94:952-959.)

Key Words: gene therapy ■ heart block ■ ion channels ■ pacemakers ■ stem cells

Although electronic pacemakers are currently the mainstay of therapy for heart block and other electrophysiological abnormalities, they are not optimal. Among their shortcomings are limited battery life, the need for permanent catheter implantation into the heart, and lack of response to autonomic neurohumors.¹ For these reasons, several gene therapy approaches have been explored as potential alternatives. These include either overexpression of β_2 -adrenergic receptors,^{2,3} use of a dominant-negative construct to suppress inward rectifier current when expressed together with the wild-type gene Kir2.1,⁴ and implantation of vectors carrying the pacemaker gene, HCN2, into atrium⁵ or bundle branch system.⁶ A problem inherent in some of these approaches²⁻⁶ is the use of viruses to deliver the necessary genes. Although the vectors have been replication-deficient adenoviruses that have little infectious potential, these incorporate the possibility of only a transient improvement in pacemaker function as

well as potential inflammatory responses. The use of retroviruses and other vectors, although not attempted as yet for biological pacemakers, carries a risk of carcinogenicity and infectivity that is unjustified, given the current success of electronic pacemakers. Attempts to use embryonic human stem cells to create pacemakers are still in their infancy and carry the problems of identifying appropriate cell lineages, the possibility of differentiation into lines other than pacemaker cells, and potential for neoplasia (see overview⁷).

With this in mind, we embarked on a project to test proof-of-principle that genetically engineered adult human mesenchymal stem cells (hMSCs) can serve as a platform for carrying the pacemaker gene to the heart. We did this with the understanding that the potential for differentiation into other cell lines exists for hMSCs as for embryonic stem cells, but with the rationale that if the relevant gene is genetically overexpressed then the presence or absence of differentiation

Original received September 22, 2003; resubmission received December 17, 2003; revised resubmission received February 11, 2004; accepted February 12, 2004.

From the Institute of Molecular Cardiology, Departments of Physiology and Biophysics (I.P., Z.L., V.V., S.D., J.Z., J.G., Z.P., P.R.B., I.S.C.), SUNY Stony Brook, Stony Brook, NY; Center for Molecular Therapeutics, Department of Pharmacology (A.P., P.D., J.Q., I.N.S., R.B.R., M.R.R.), Department of Pediatrics (M.R.R.), and the Institute of Comparative Medicine and Department of Pathology (A.J.H.), Columbia University, New York, NY.

*Both authors contributed equally to this study.

This manuscript was sent to Harry A. Fozzard, Consulting Editor, for review by expert referees, editorial decision, and final disposition.

Correspondence to Michael R. Rosen, MD, Center for Molecular Therapeutics, Depts of Pharmacology and Pediatrics, Columbia University, 630 West 168 St, PH 7West-321, New York, NY 10032. E-mail mrr1@columbia.edu

© 2004 American Heart Association, Inc.

Circulation Research is available at <http://www.circresaha.org>

DOI: 10.1161/01.RES.0000123827.60210.72

may be less important. Further, in testing proof-of-principle, we did not attempt to test the long-term safety of engineered hMSCs, which has yet to be demonstrated.

In this study, we demonstrate that hMSCs are effectively transfected by electroporation with a vector construct directing the expression of mouse HCN2 (mHCN2) as well as EGFP, and are capable of expressing functional mHCN2 channels in vitro. HCN2 expression in hMSCs provides an I_f -based current sufficient to change the beating rate of cocultured neonatal rat ventricular myocytes, and to drive the canine ventricle, mimicking the HCN2 overexpression by adenoviral constructs.⁵ We demonstrate that hMSCs make connexin proteins and form functional gap junctions that couple electrically with canine cardiac myocytes. Thus, we have developed an ex vivo gene therapy system using genetically modified hMSCs as a platform for delivery of pacemaker genes into the heart.

Materials and Methods

Protocols were reviewed and approved by the Columbia University institutional animal care and use committee.

Human Mesenchymal Stem Cell Maintenance and Transfection

Human mesenchymal stem cells (Poietics hMSC; mesenchymal stem cells, human bone marrow) were purchased from Clonetics/BioWhittaker (Walkersville, Md) and cultured in MSC growing medium (Poietics MSCGM; BioWhittaker) at 37°C in a humidified atmosphere of 5% CO₂. Cells were used from passages 2 to 4. A full-length mHCN2 cDNA was subcloned into a pIRES2-EGFP vector (BD Biosciences Clontech). Cells were transfected by electroporation using the Amaxa Biosystems Nucleofector (Amaxa) technology.⁸ Expression of EGFP after 24 to 48 hours revealed transfection efficiency of 30% to 45%.

Patch-Clamp Studies of I_{HCN2} Expressed in hMSCs

We used whole-cell patch clamp to study membrane currents in control hMSCs and those transfected with mHCN2, the gene encoding the α -subunit of the pacemaker current, I_f . Expressed I_f (ie, I_{HCN2}) was measured under voltage-clamp by an Axopatch-1B (Axon Instruments) amplifier. Patch electrode resistance was 4 to 6 M Ω before sealing. Cells were constantly superfused using a gravitational perfusion system with a complete change of the chamber solutions in about 0.5 minutes. The temperature of the bath as well as of the perfusion solution was kept constant at 35 \pm 0.5°C. The pipette solution was filled with (in mmol/L) KCl 50, K-aspartate 80, MgCl₂ 1, Mg-ATP 3, EGTA 10, and HEPES 10 (pH adjusted to 7.2 with KOH). The external solution contained (in mmol/L) NaCl 137.7, KCl 5.4, NaOH 2.3, CaCl₂ 1.8, MgCl₂ 1, Glucose 10, HEPES 5, and BaCl₂ 2 (pH adjusted to 7.4 with NaOH). The membrane capacity was measured by applying a voltage clamp step and current densities are expressed as the value of peak current per capacity.

Dual Patch-Clamp Studies of Gap Junctions

Canine cardiac ventricular myocytes were isolated as previously described.⁹ Primary cultures of the myocytes were maintained using procedures described for mouse myocytes.¹⁰ They were plated at 0.5 to 1 \times 10⁴ cells/cm² in MEM containing 2.5% fetal bovine serum (FBS) and 1% PS onto mouse laminin (10 μ g/mL) precoated coverslips. After 1 hour of culture in a 5% CO₂ incubator at 37°C, the medium was changed to FBS-free MEM. hMSCs were added and coculture was maintained in DMEM with 5% FBS. Cell Tracker green (Molecular Probes) was used to distinguish hMSCs from HeLa cells in coculture in all experiments.¹¹

Glass coverslips with adherent cells were transferred to an experimental chamber perfused at room temperature (\approx 22°C) with

bath solution containing (in mmol/L) NaCl 150, KCl 10, CaCl₂ 2, HEPES 5 (pH 7.4), and glucose 5. The patch pipettes were filled with solution containing (in mmol/L) K⁺ aspartate⁻ 120, NaCl 10, MgATP 3, HEPES 5 (pH 7.2), and EGTA 10 (pCa \approx 8), filtered through 0.22- μ m pores. When filled, the resistance of the pipettes measured 1 to 2 M Ω . Experiments were performed on cell pairs using a double voltage-clamp. This method permitted us to control the membrane potential (V_m) and measure the associated junctional currents (I_j).

Action Potential Recordings in Coculture

hMSCs were plated onto fibronectin-coated 9 \times 22-mm coverslips, using a cloning cylinder to restrict the initial plating to an approximate 4-mm diameter circular area. The cells expressed either EGFP alone or EGFP+mHCN2. Four hours later, the cloning cylinder was removed and neonatal rat ventricular myocytes, prepared as described previously,¹² were plated over the entire coverslip. Four to five days later, the coverslips were placed in a superfusion chamber maintained at 35°C and action potentials recorded from near the center of the coverslip using a perforated patch electrode¹² and normal physiological solution containing (in mmol/L) NaCl 140, NaOH 2.3, MgCl₂ 1, KCl 5.4, CaCl₂ 1.0, HEPES 5, and glucose 10; pH 7.4. Pipette solution included (in mmol/L) aspartic acid 130, KOH 146, NaCl 10, CaCl₂ 2, EGTA-KOH 5, Mg-ATP 2, and HEPES-KOH 10; pH 7.2. Recordings were conducted with an Axopatch 200 amplifier and PClamp 8 software (Axon Instruments). The perforated patch technique was used, and amphotericin B (400 μ g/mL, Sigma) was added to the pipette solution.

In Vivo Studies in Canine Ventricle

Stem cells were prepared as above. Under sterile conditions, after sodium thiopental induction (17 mg/kg IV) and inhalational isoflurane (1.5 to 2.5%) anesthesia, 23- to 27-kg mongrel dogs (Team Associates, Dayville, Conn) were subjected to a pericardiectomy. We injected 10⁶ hMSCs containing HCN2+GFP or GFP alone subepicardially in 0.6 mL of solution into the left ventricular anterior wall, approximately 2 mm deep to the epicardium via a 21-gauge needle. Animals recovered for 4 to 10 days, during which their cardiac rhythms were monitored. They then were anesthetized with isoflurane, as above. Both cervical vagal trunks were isolated, the chest opened, and ECGs monitored. Graded right and left vagal stimulation was performed via standard techniques¹³ to suppress sinus rhythm such that escape pacemaker function might occur. Tissues were then removed for histological study.

Histological Methods

Unless otherwise indicated, samples of heart tissue were fixed in 10% buffered formalin, embedded in paraffin and sectioned at 4 or 6 micrometers. Some formalin-fixed sections were stained in a routine fashion with hematoxylin and eosin (H&E). Monoclonal mouse antibodies (DakoCytomation) raised against the vimentin and human CD 44 were used applying an avidin-biotin-peroxidase method.¹⁴ Tissues stained immunohistochemically were then counterstained with hematoxylin. We used positive and negative controls for immunohistochemical staining. hMSCs were distinguished from fibroblasts by CD 44 staining. The vimentin antibody intensely stains hMSCs but also stains most mesenchymal tissue. Other sections were treated to remove wax and rehydrated by exposure to xylene for 6 minutes with three rinses followed by similar exposures to 100%, 95%, 50% ethanol, deionized water, and PBS. The sections were then exposed to 30% hydrogen peroxide for 10 minutes and were again rinsed in PBS for 50 minutes. The rehydrated sections were exposed to a 0.01 mol/L citrate buffer, which was heated to a boil for 10 minutes and then allowed to cool to room temperature. Polyclonal antibodies raised against connexin 43 (Cx43; Zymed Laboratories Inc) were used.

Statistics

Results are presented as mean \pm SEM. Statistical significance was determined by Student's *t* test for unpaired data. A value of *P*<0.05 was considered significant.

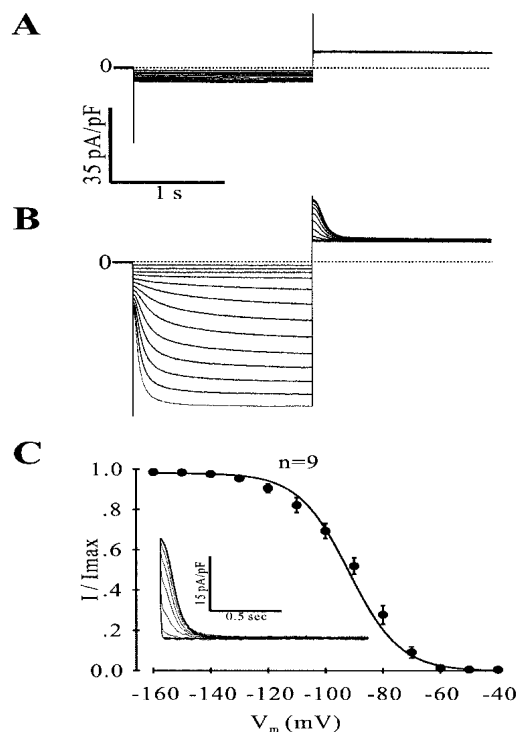


Figure 1. Functional expression of I_f in hMSCs transfected with mHCN2 gene. I_f was expressed in hMSCs transfected with the mHCN2 gene (B) but not in nontransfected stem cells (A). C, Fit by the Boltzmann equation to the normalized tail currents of I_f gives a midpoint of -91.8 ± 0.9 mV and a slope of 8.8 ± 0.5 mV ($n=9$). I_f was fully activated around -140 mV with an activation threshold of -60 mV. Inset shows representative tail currents used to construct I_f activation curves. Voltage protocol was to hold at -30 mV and hyperpolarize for 1.5 seconds to voltages between -40 and -160 mV in 10-mV increments followed by a 1.5-second voltage step to $+20$ mV to record the tail currents.

Results

Transfection of hMSCs With mHCN2 and Demonstration of Pacemaker Current

Nontransfected hMSCs demonstrated no significant time-dependent currents during hyperpolarizations (Figure 1A). MHCN2-transfected hMSCs expressed a large time-dependent inward current activating on hyperpolarizations up to -160 mV and deactivating during the following step to 20 mV (Figure 1B). Figure 1C shows the I_f activation curve constructed from tail currents recorded in mHCN2-transfected hMSCs (see inset for sample currents). We fit the data with a Boltzmann two-state model, which yielded a midpoint (V_{50}) of -91.8 ± 0.9 mV and a slope factor of 8.8 ± 0.5 mV ($n=9$), similar to values for mHCN2 expression in oocytes and HEK 293 cells.^{15,16} These values are an approximation because the I_f current density was large and its slow rundown was apparent, as in all other preparations. The results suggest I_f should be activated at diastolic potentials in the hMSCs if they are well coupled by gap junctions to ventricular myocytes. To confirm the expressed current was I_f , we executed the experiments illustrated in Figure 2. The voltage protocol (see Figure 2 legend for description) allowed us to determine the reversal potential of -37.5 ± 1.0 mV ($n=8$). Given the extracellular $[K^+]$ of 5.4 mmol/L, this

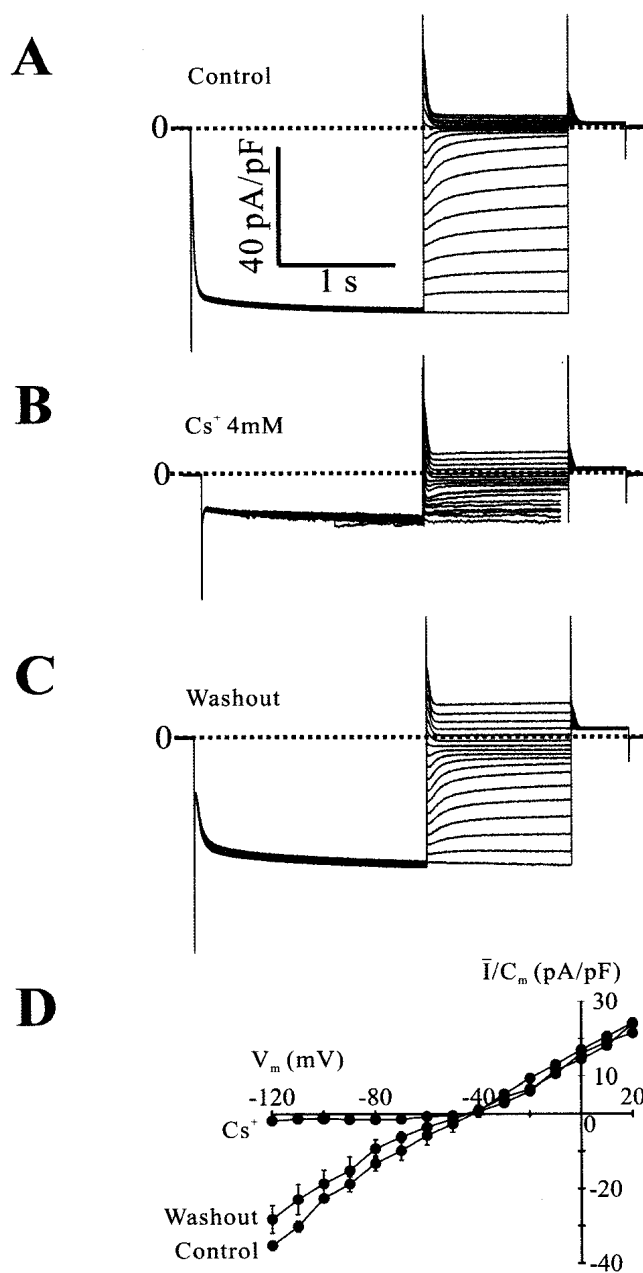


Figure 2. Effect of extracellular application of Cs^+ and measurement of the reversal potential of I_f . I_f was recorded before (A), during (B), and after (C) external addition of 4 mmol/L Cs^+ . D, Fully activated I - V relationship of I_f in the absence and presence of Cs^+ . Voltage protocol was to hold at -30 mV and hyperpolarize to -150 mV for 2 seconds followed by a 1.5-second depolarization to voltages between -150 and $+20$ mV to record the tail currents necessary to construct the fully activated current-voltage relation followed by a 0.5-second step to -10 mV.

reversal potential is consistent with the mixed selectivity of the I_f channel to $[Na^+]$ and $[K^+]$.¹⁷ We also tested the effect of Cs^+ to block the expressed current. Cs^+ (4 mmol/L) reversibly blocked the inward currents but had little effect on the outward deactivating tail currents, consistent with Cs^+ blockade of I_f .¹⁸ We constructed the fully activated I - V relationships for the I_f -like current in Figure 2D. The plot reinforces the two major observations from the raw data.

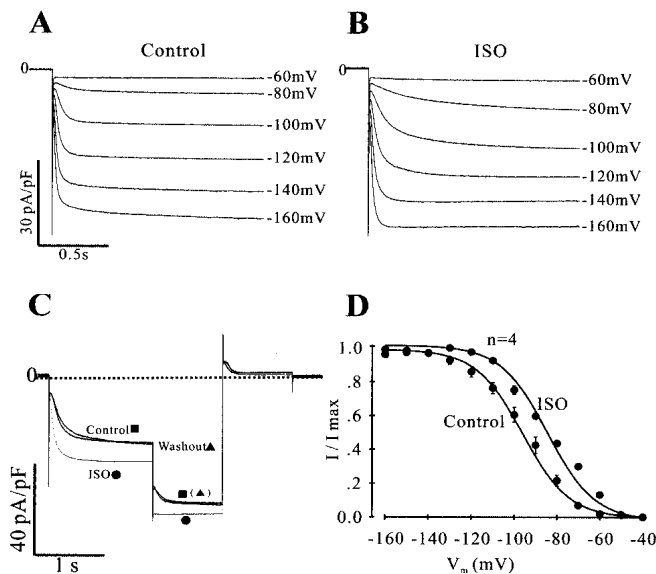


Figure 3. Modulation of I_f activation by isoproterenol (ISO) in hMSCs transfected with the mHCN2 gene. I_f activation in the absence (A) and presence of ISO, 1×10^{-6} mol/L (B). C, Voltage dependence of activation of I_f in control, ISO, and washout using a two-step pulse protocol. D, Boltzmann fit to the normalized density of tail currents. Activation curve was constructed with the same protocol as in Figure 1. Two-pulse protocol was initiated from a holding potential of -30 mV. First step was to -100 mV for 1.5 seconds followed by a second step to -150 mV for 1 second. Voltage was then stepped to $+15$ mV for 1 second to rapidly deactivate the current and then returned to the holding potential.

First, inward but not outward I_f -like currents are blocked by Cs^+ , and second, the zero current indicates a mixed selectivity consistent with the known properties of I_f . In a separate protocol I_f density at -150 mV was 31.1 ± 3.8 pA/pF ($n=17$). Membrane capacity for the transfected hMSCs was 110.8 ± 9.0 pF ($n=17$).

Neurohumoral Regulation of I_{HCN2}

A potential advantage of biological over electronic pacemakers is their hormonal regulation. We therefore examined the effects of β -adrenergic and muscarinic agonists on I_f recorded in the hMSCs (Figures 3 and 4). Figures 3A and 3B demonstrate that the currents at -80 and -100 mV in isoproterenol are larger than those in control, whereas the currents in both conditions are almost equal at -160 mV. This voltage-dependent difference is expected for a shift in the activation curve (Figure 3D). The half activation voltage (V_{50}) was -96 ± 0.9 mV in control and -84.4 ± 0.2 mV in isoproterenol ($n=4$, $P<0.01$). The slope factor was 10.9 ± 0.5 mV in control and 11.0 ± 0.2 mV in isoproterenol ($P>0.05$). Using a two-pulse protocol to illustrate the shift in activation, the time-dependent current in the presence of isoproterenol is larger in response to the first step than control and smaller in response to the second step (Figure 3C). This is consistent with an ISO-induced positive shift in I_f activation. Acetylcholine had no direct effect on the time-dependent current ($n=3$), due either to the absence of muscarinic receptors or to a low basal level of cAMP that could not be further reduced by acetylcholine inhibition of adenylyl cyclase. We therefore

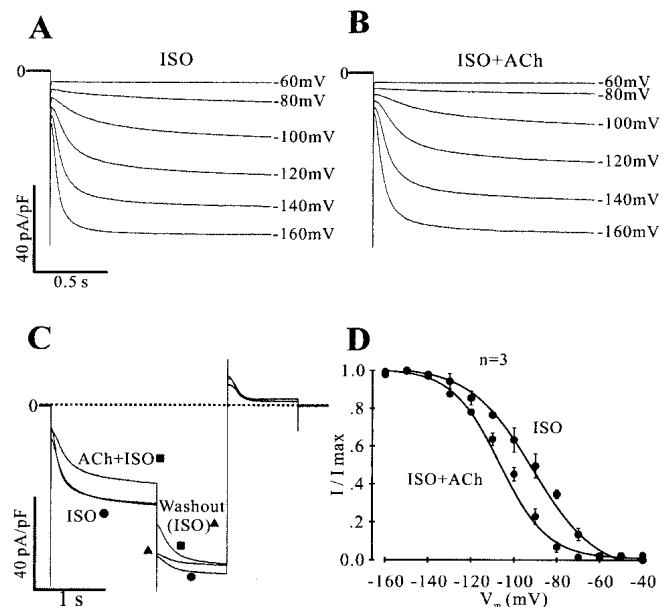


Figure 4. Modulation of I_f activation by acetylcholine (ACh) in the presence of ISO. I_f activation in the presence of ISO and in the absence (A) and presence (B) of ACh (1×10^{-6} mol/L). C, Same two-step protocol as in Figure 3C, for ISO (1×10^{-6} mol/L) alone and ISO+ACh. D, Boltzmann fit to normalized currents. Activation curve was constructed with the same protocol as in Figure 1.

further tested whether acetylcholine could reverse the actions of isoproterenol (Figure 4). Examination of the response to the step hyperpolarizations to -80 and -100 mV indicate that addition of acetylcholine reduces the membrane currents. However, they are almost identical at -160 mV (Figures 4A and 4B), consistent with a negative shift in activation induced by acetylcholine. Figure 4D shows the activation curves in isoproterenol and isoproterenol+acetylcholine. The V_{50} s were -91.3 ± 1.1 mV for isoproterenol and -106.6 ± 0.8 mV for isoproterenol+acetylcholine ($n=3$, $P<0.05$). The slope factors were 14.6 ± 0.9 mV in isoproterenol and 11.1 ± 0.9 mV ($n=3$, $P<0.05$). We also used a two-pulse protocol (Figure 4C). The response to the first voltage step is larger in isoproterenol than in isoproterenol+acetylcholine, whereas the reverse is true for the second step. This is again consistent with a negative shift in activation induced by addition of acetylcholine. These results demonstrate that the hMSCs transfected with mHCN2 should respond to β -adrenergic and muscarinic agonists.

mHCN2-Transfected hMSCs Modulation of Impulse Initiation by Cardiac Myocytes

Having expressed the pacemaker gene in hMSCs, we hypothesized that the mHCN2-transfected hMSCs could influence excitability of coupled heart cells. Maximum diastolic potential was -74 ± 1 mV ($n=5$) in neonatal rat ventricular myocytes cocultured with EGFP expressing hMSCs and -67 ± 2 mV ($n=6$) in myocytes cocultured with hMSCs expressing mHCN2 ($P<0.05$). Spontaneous rate was 93 ± 16 bpm in the former group ($n=5$) and 161 ± 4 bpm in the latter ($n=6$, $P<0.05$). The reduced maximum diastolic potential is consistent with the observed threshold potential of the ex-

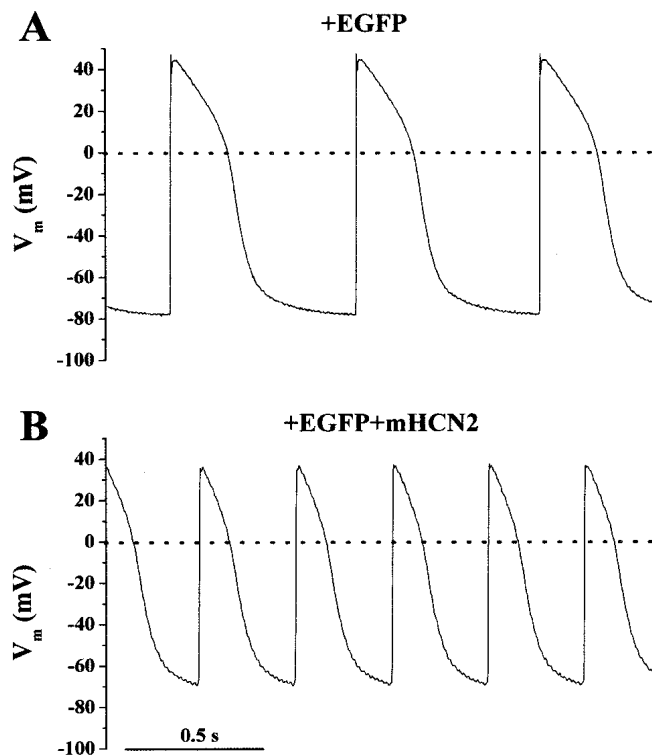


Figure 5. Pacemaker function in in vitro model. Spontaneous electrical activity of neonatal rat ventricular myocytes cocultured for 4 to 5 days with hMSCs transfected with EGFP alone (A) or mHCN2 and EGFP (B). Experiments were conducted at 35°C.

pressed current in the mHCN2-transfected hMSCs, and indicates the influence of this depolarizing current on the electrically coupled myocytes. Representative action potentials are shown in Figure 5.

mHCN2-Transfected hMSCs as a Biological Pacemaker in Intact Canine Heart

Given the demonstration of functional coupling of mHCN2-expressing hMSCs to myocytes in vitro, we then injected them into canine heart in situ (see Materials and Methods) to test whether pacemaker function was demonstrable. During sinus arrest, escape pacemaker function can originate in the left or right ventricle, as occurred here, with two of four

animals receiving hMSCs expressing EGFP alone developing left and two developing right ventricular escape rhythms. In contrast, five of six animals receiving hMSCs expressing EGFP+mHCN2 developed rhythms originating from and pace-mapped to the left ventricle at a site whose origin approximated that of the hMSC injection. Moreover, the idioventricular rates of these animals was 61 ± 5 versus 45 ± 1 bpm in animals receiving hMSCs expressing EGFP alone ($P < 0.05$). A representative experiment is shown in Figure 6.

Hematoxylin and eosin stain of the site of hMSCs injection revealed normal cardiac myocytes and dense areas of basophilic infiltration adjacent to the needle track (Figure 7A). The hMSCs were easily identified by their size (10 to 20 μm in diameter), large hyperchromatic nuclei, and scanty, deeply basophilic cytoplasm with no matrix. Although the hMSCs had a characteristic appearance with H&E staining, they were more precisely identified by using immunohistochemical stains. The hMSCs stained intensely for vimentin (eg, Figure 7B), a marker of cells of mesenchymal origin. The same regions also were positive for human CD44 (eg, Figure 7C). Interdigitation between hMSCs and myocardium was very clear (eg, Figure 7D).

hMSCs Form Gap Junctions With Cardiac Myocytes In Vitro and In Vivo

To test whether the hMSCs couple electrically with cardiac myocytes, we cocultured hMSCs with adult canine ventricular myocytes. Myocytes were dissociated and plated for between 12 and 72 hours before coculture with hMSCs. Measurement of coupling occurred 6 to 12 hours after adding hMSCs to the myocyte culture. Our preliminary observations reveal that stem cells couple to cardiac cells. Figure 8A illustrates one example of an hMSC-myocyte pair in coculture; it is one of four so far observed. For heterologous pairs identification the hMSCs were tagged with Cell Tracker green (Molecular Probes).¹¹ A bipolar voltage-ramp protocol was used to alter transjunctional voltage V_j ($V_2 - V_1$) over ± 100 mV range at 200 mV/15-second rate (see V_1 and V_2) and is shown in Figure 8B. The ramp pulse was applied to the myocyte (V_1) while membrane potential of the hMSC was kept at 0 mV (V_2). The associated sister currents, I_1 and I_2 , were recorded from the myocyte and hMSC, respectively.

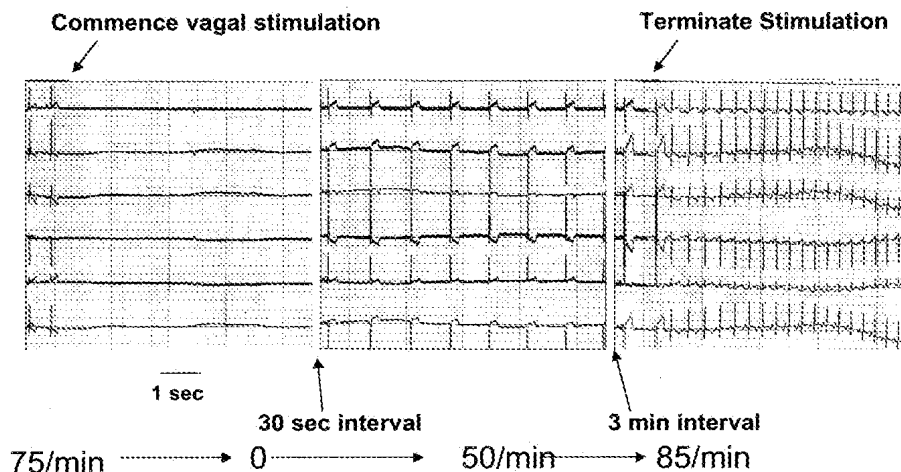


Figure 6. Pacemaker function in canine heart in situ. Top to bottom, ECG leads I, II, III, AVR, AVL, and AVF. Left, Last two beats in sinus rhythm and onset of vagal stimulation (arrow) causing sinus arrest in a dog studied 7 days after implanting mHCN2-transfected hMSCs in LV anterior wall epicardium. Middle, During continued vagal stimulation, an idioventricular escape focus emerges, having a regular rhythm. Right, On cessation of vagal stimulation (arrow), there is a postvagal sinus tachycardia.

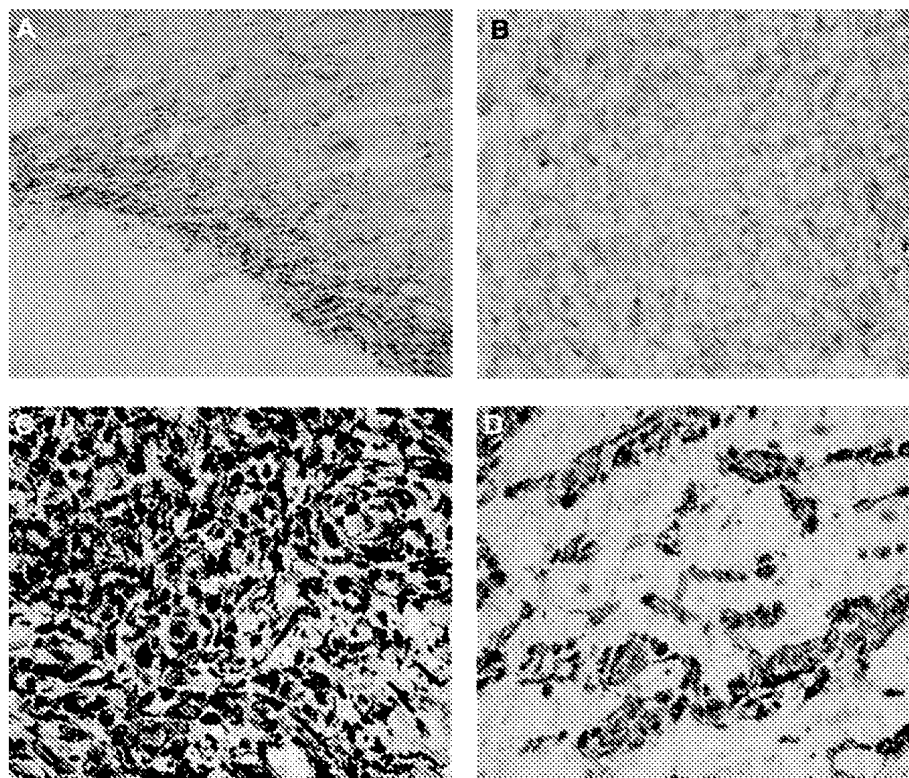


Figure 7. A, H&E stain showing basophilic-stained stem cells and normal myocardium. B and C show, respectively, vimentin and CD44 staining of a node of hMSCs in canine myocardium. D, Detail of vimentin-stained cells interspersed with myocardium. Magnification $\times 100$ (A) and $\times 400$ (B through D).

The currents followed the voltage-ramp profile demonstrating gap junction coupling of the heterologous hMSC-myocyte pair. The current, I_2 , obtained from the nonstepped hMSC, reflects a coupling current, I_j . This record demonstrates effective coupling of the hMSC to the ventricular myocyte. Figure 8C shows immunohistochemical staining with anti-Cx43 antibodies of the site of the injection of hMSCs into the canine heart. Intercalated discs are revealed in the myocardium (see purple arrow), whereas small punctate staining for Cx43 is seen between hMSCs (white arrows). There is also Cx43 staining at interfaces between hMSCs and myocytes (red arrows). The inset of Figure 8C shows a section from a piece of myocardium (fixed in 4% paraformaldehyde in 0.1 mol/L phosphate buffer at pH of 7.4 at 4°C and subsequently treated as described by Walcott et al¹⁹) injected with hMSCs expressing EGFP plus HCN2. The red staining from the secondary antibody to EGFP illustrates localization of hMSCs, whereas the blue staining illustrates cell nuclei. A significant majority of the clustered cells are hMSCs.

Discussion

Pacemaker implantation is a primary treatment for complete heart block or sinus node dysfunction. The current therapy uses electronic devices with high reliability and low morbidity. Nevertheless, such devices are not optimal because they lack the biological responsiveness of native tissues. Recently several approaches have been attempted to provide biological pacemaker function. Included among these attempts have been an upregulation of β_2 -adrenergic receptors, a downregulation of the background K^+ current I_{K1} and our own previous studies with overexpression of the HCN2 gene, the molecular correlate of the endogenous cardiac pacemaker current I_f .²⁻⁶

In these latter studies, we showed that HCN2 overexpression locally in left atrium or in the proximal bundle-branch system induces both I_f -like currents and in situ pacemaker function in the recipient myocytes. The unique voltage dependence of the I_f conductance results in current flow during diastole but not during the action potential plateau, limiting possible complications attendant to significant alterations of the action potential waveform. Although an adenoviral construct has been used to deliver the HCN2 gene to the heart,^{5,6} this approach is not optimal because adenoviruses are episomal and the nucleic acids they deliver do not integrate into genome. Other viral systems are accompanied by a number of serious drawbacks that hinder their use in vivo.

An alternative means for fabricating biological pacemakers is via embryonic stem cells, which can be differentiated along a cardiac lineage and might provide a platform for cell-based control of cardiac rhythm. Embryonic stem cells can make functional gap junctions and generate spontaneous electrical activity.²⁰ However because of their immunogenicity, rejection is a serious consideration. Moreover, as with hMSCs, embryonic stem cell preparations are not spatially uniform and the proper engineering of both cell-based systems presents a challenge in designing in vivo biological pacemakers.

For several reasons, hMSCs are an attractive cellular vehicle for gene delivery applications. They can be obtained in relatively large numbers through a standard clinical procedure. hMSCs are easily expanded in culture and capable of long-term transgene expression.²¹ Their administration can be autologous or via banked stores, given evidence that they may be immunoprivileged.²² Long-term function of such a pacemaker is based on prolonged expression of mHCN2, which in turn requires integration into the genome of hMSCs. Random

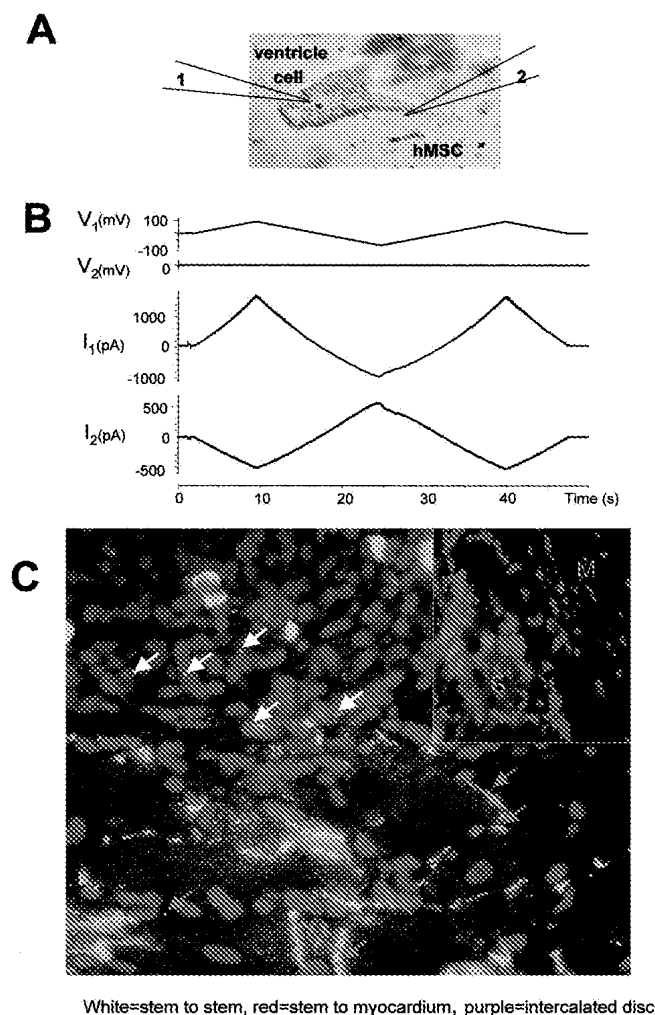


Figure 8. Gap junctions between an hMSC-canine ventricular myocyte pair. **A**, Phase-contrast micrograph of a hMSC-myocyte pair and locations of pipettes 1 and 2. **B**, Voltage ramp ($V_1 = \pm 100$ mV; $V_2 = 0$) applied to the canine myocyte evoked current flow through the patch pipettes attached in whole-cell mode to the myocyte, I_1 , and hMSC, I_2 . Currents recorded from the stepped myocyte, I_1 , represent the sum of two components, a junctional current and a membrane current in the myocyte. The mirror current, I_2 , recorded from the nonstepped hMSC corresponds to the junctional current, I_j , between the hMSC-myocyte pair. **C**, Immunostaining for Cx43 in a region of interface between an injection site and myocardium. DAPI staining reveals nuclei. Arrows are purple, intercalated discs; white, Cx43 staining between hMSCs; red, Cx43 staining between hMSCs and myocytes. Inset, DAPI and EGFP antibody staining of a section from another animal, which was subjected to para-formaldehyde fixation and immunostained with anti-EGFP and DAPI to verify that injection sites contained hMSCs. M indicates myocardium; S, hMSC.

integration increases the possibility of disruption of genes involved in the cell cycle or tumor suppression, or may cause epigenetic changes. However, the *ex vivo* transfection method used here allows the DNA integration site to be evaluated before use and the cell carriers can be engineered with fail-safe death mechanisms.

The objective of this study was to test the feasibility of using genetically modified hMSCs as a platform for systemic delivery of pacemaker genes into the heart. HCN2 served as

the model system for this study. Our genetically engineered hMSCs expressed an I_f -like current and were capable of increasing the spontaneous beating rate of cocultured rat neonatal myocytes and originating a ventricular rhythm during vagally induced sinus arrest in the canine heart. Control hMSCs expressing only EGFP did not exert these effects either *in vitro* or *in vivo*. Thus, the electrical effects of the hMSCs transfected with the mHCN2 gene were similar to the effects of overexpression of the same gene in the myocytes in *in vitro* and *in vivo* systems. These findings suggest that hMSCs may serve as an alternative approach for the delivery of pacemaker genes for cardiac implantation.

In sinus node myocytes the HCN gene generates an inward current necessary for cardiac excitation. Unlike sinoatrial node cells, mHCN2-transfected hMSCs are not excitable, because they lack the other currents required to generate an action potential. However, these cells are able to generate a depolarizing current, which spreads to coupled myocytes, driving myocytes to threshold. Our hypothesis is that as long as the hMSCs contain the pacemaker gene and couple to cardiac myocytes via gap junctions, they will function as a cardiac pacemaker in an analogous manner to the normal primary pacemaker the sinoatrial node. We demonstrated using dual patch technique that hMSCs form gap junctions that couple electrically with canine cardiac myocytes. The coupling between engrafted hMSCs and cardiac myocytes was also shown by immunohistochemical staining of the tissues isolated from the site of hMSC injection using anti-connexin 43 antibodies. Within an injection site, the clusters of cells were vimentin and CD44 positive, and we also demonstrated that a significant majority of the cluster of cells were EGFP positive, thereby confirming their identity as hMSCs. A recent report has suggested that mouse MSCs can fuse with mouse myocytes *in vivo* with a fusion rate of 0.005%.²³ We have not ruled this possibility out in our studies, but at the fusion rate reported by Morimoto et al,²³ only 50 hMSCs of the million cells injected would fuse.

There are limitations to the approach used in this study. First, the hMSCs were delivered to the free wall myocardium, not an optimal site for ordered contraction. However, we have recently used catheter approaches to insert pacemaker genes into the canine left bundle branch system.⁶ Such a locus offers the possibility of more ordered and normal activation and contraction than is the case with a pacemaker residing in the free wall. Before this approach is used for hMSCs, catheter modification may need to occur to optimize injection of cells of the size of an hMSC without cell injury or destruction.

Another question relates to the duration of efficacy of these pacemakers. In the present study, we were only concerned with demonstrating the feasibility of using hMSCs as a gene delivery system. Because our studies *in vivo* lasted only 3 to 10 days, transient transfections were sufficient. Before this approach can be considered clinically relevant, far longer periods of study will be required. In this regard, our transfected cells maintain their green fluorescence for at least 3 months when grown on antibiotic to select stably expressing cells. This indicates that we have selected for stable clones expressing mHCN2, so it is likely that persistence of expression will not pose significant difficulties for more prolonged

studies. However, it remains to be determined if the differentiation state of the hMSCs is altered in situ in the long term, or whether such differentiation would affect mHCN2 expression or biophysical properties. In addition, a murine gene, which is quite close but not completely identical in sequence to the human gene was used here. Not only would it be most advantageous to use human genes, but the exploration of various mutations to optimize activation and recovery characteristics, as well as neurohumoral response would be desirable. Such approaches are currently being explored.

In closing, the delivery of hMSCs expressing mHCN2 to the canine heart is not only a demonstration of feasibility of preparing hMSC-based biological pacemakers, but is the first concrete example of a general principle: hMSCs can be used to deliver a variety of genes to influence the function of syncytial tissues. One alternative potential cardiovascular application is delivery of K^+ channel genes to hyperpolarize vascular smooth muscle inducing relaxation. Indeed, the payload delivered by hMSCs need not be restricted to membrane channels: any gene product or small molecule that can permeate gap junctions (MW <1000, minor diameter <1.2 nm) can be incorporated into the hMSCs and delivered to a syncytial tissue as its therapeutic target.

Acknowledgments

This work was supported by US Public Health Service National Heart, Lung, and Blood Institute grants HL-28958, HL-67101, HL-20558, and GM-55263. We would like to acknowledge Dr Sandy Ambrus in the Department of Pathobiology at Texas A&M for performing some immunohistochemical stainings. In addition, our thanks to Eileen Franey for her careful attention to the preparation of the manuscript.

References

1. Zivin A, Bardy GH. Cardiac pacemakers. In: Spooner PM, Rosen MR, eds. *Foundations of Cardiac Arrhythmias*. New York, NY: Marcel Dekker, Inc; 2001;571–598.
2. Edelberg JM, Aird WC, Rosenberg RD. Enhancement of murine cardiac chronotropy by the molecular transfer of the human β_2 -adrenergic receptor cDNA. *J Clin Invest*. 1998;101:337–343.
3. Edelberg JM, Huang DT, Josephson ME, Rosenberg RD. Molecular enhancement of porcine cardiac chronotropy. *Heart*. 2001;86:559–562.
4. Miake J, Marban E, Nuss HB. Gene therapy: biological pacemaker created by gene transfer. *Nature*. 2002;419:132–133.
5. Qu J, Plotnikov AN, Danilo P Jr, Slapakova I, Cohen IS, Robinson RB, Rosen MR. Expression and function of a biological pacemaker in canine heart. *Circulation*. 2003;107:1106–1109.
6. Plotnikov AN, Sosunov EA, Qu J, Shlapakova I, Anyukhovsky EP, Liu L, Janse MJ, Brink PR, Cohen IS, Robinson RB, Danilo P Jr, Rosen MR. A biological pacemaker implanted in the canine left bundle branch provides ventricular escape rhythms having physiologically acceptable rates. *Circulation*. 2004;109:506–512.
7. Gepstein L. Derivation and potential applications of human embryonic stem cells. *Circ Res*. 2002;91:866–876.
8. Hamm A, Krott N, Breibach I, Blindt R, Bosserhoff AK. Efficient transfection method for primary cells. *Tissue Eng*. 2002;8:235–245.
9. Yu H, Gao J, Wang H, Wymore R, Steinberg S, McKinnon D, Rosen MR, Cohen IS. Effects of the renin-angiotensin system on the current I_{to} in epicardial and endocardial ventricular myocytes from the canine heart. *Circ Res*. 2000;86:1062–1068.
10. Zhou YY, Wang SQ, Zhu WZ, Chruscinski A, Kobilka BK, Ziman B, Wang S, Lakatta EG, Cheng H, Xiao RP. Culture and adenoviral infection of adult mouse cardiac myocytes: methods for cellular genetic physiology. *Am J Physiol (Heart Circ Physiol)*. 2000;279:H429–H436.
11. Valiunas V, Weingart R, Brink PR. Formation of heterotypic gap junction channels by connexins 40 and 43. *Circ Res*. 2000;86:e42–e49.
12. Protas L, Robinson RB. Neuropeptide Y contributes to innervation-dependent increase in I_{CaL} via ventricular Y2 receptors. *Am J Physiol*. 1999;277:H940–H946.
13. Rosenshtraukh L, Danilo P Jr, Anyukhovsky EP, Steinberg SF, Rybin V, Brittain-Valenti K, Molina-Viamonte V, Rosen MR. Mechanisms for vagal modulation of ventricular repolarization and of coronary occlusion-induced lethal arrhythmias in cats. *Circ Res*. 1994;75:722–732.
14. Hsu S, Raine L. Protein A, avidin, and biotin in immunohistochemistry. *J Histochem Cytochem*. 1981;29:1349–1353.
15. Yu H, Wu J, Potapova I, Wymore RT, Holmes B, Zuckerman J, Pan Z, Wang H, Shi W, Robinson RB, El-Maghrabi MR, Benjamin W, Dixon J, McKinnon D, Cohen IS, Wymore R. MinK-related peptide 1: A β subunit for the HCN ion channel subunit family enhances expression and speeds activation. *Circ Res*. 2001;88:e84–e87.
16. Moosmang S, Stieber J, Zong X, Biel M, Hofmann F, Ludwig A. Cellular expression and functional characterization of four hyperpolarization-activated pacemaker channels in cardiac and neuronal tissues. *Eur J Biochem*. 2001;268:1646–1652.
17. DiFrancesco D. A study of the ionic nature of the pacemaker current in calf Purkinje fibres. *J Physiol*. 1981;314:377–393.
18. DiFrancesco D. Block and activation of the pacemaker channel in calf Purkinje fibres: effects of potassium, caesium and rubidium. *J Physiol*. 1982;329:485–507.
19. Walcott B, Moore LC, Birzgalis A, Claros N, Valiunas V, Ott T, Willecke C, Brink PR. The role of gap junctions in fluid secretion of lacrimal glands. *Am J Physiol*. 2002;282:C501–C507.
20. Boheler KR, Czy J, Tweedie D, Yang HT, Anisimov SV, Wobus AM. Differentiation of pluripotent embryonic stem cells into cardiomyocytes. *Circ Res*. 2002;91:189–201.
21. Zhang XY, La Russa VF, Bao L, Kolls J, Schwarzenberger P, Reiser J. Lentiviral vectors for sustained transgene expression in human bone marrow-derived stromal cells. *Mol Ther*. 2002;5:555–565.
22. Liechty KW, MacKenzie TC, Shaaban AF, Radu A, Moseley AM, Deans R, Marshak DR, Flake AW. Human mesenchymal stem cells engraft and demonstrate site-specific differentiation after in utero transplantation in sheep. *Nat Med*. 2000;6:1282–1286.
23. Morimoto Y, Davis BH, van der Bos E-J, McMichael MD, Taylor D. Transplanted bone marrow derived mesenchymal stem cells fuse with cardiomyocytes. *Circulation*. 2003;108:IV-548. Abstract.

RAPID REPORT

Human mesenchymal stem cells make cardiac connexins and form functional gap junctions

Virginijus Valiunas¹, Sergey Doronin¹, Laima Valiuniene¹, Irina Potapova¹, Joan Zuckerman¹, Benjamin Walcott¹, Richard B. Robinson², Michael R. Rosen², Peter R. Brink¹ and Ira S. Cohen¹

¹Department of Physiology and Biophysics, Institute of Molecular Cardiology, State University of New York at Stony Brook, Stony Brook, NY 11794, USA

²Department of Pharmacology, Center for Molecular Therapeutics, Columbia University, New York, NY 10032, USA

Human mesenchymal stem cells (hMSCs) are a multipotent cell population with the potential to be a cellular repair or delivery system provided that they communicate with target cells such as cardiac myocytes via gap junctions. Immunostaining revealed typical punctate staining for Cx43 and Cx40 along regions of intimate cell-to-cell contact between hMSCs. The staining patterns for Cx45 rather were typified by granular cytoplasmic staining. hMSCs exhibited cell-to-cell coupling to each other, to HeLa cells transfected with Cx40, Cx43 and Cx45 and to acutely isolated canine ventricular myocytes. The junctional currents (I_j) recorded between hMSC pairs exhibited quasi-symmetrical and asymmetrical voltage (V_j) dependence. I_j records from hMSC–HeLaCx43 and hMSC–HeLaCx40 cell pairs also showed symmetrical and asymmetrical V_j dependence, while hMSC–HeLaCx45 pairs always produced asymmetrical I_j with pronounced V_j gating when the Cx45 side was negative. Symmetrical I_j suggests that the dominant functional channel is homotypic, while the asymmetrical I_j suggests the activity of another channel type (heterotypic, heteromeric or both). The hMSCs exhibited a spectrum of single channels with transition conductances (γ_j) of 30–80 pS. The macroscopic I_j obtained from hMSC–cardiac myocyte cell pairs exhibited asymmetrical V_j dependence, while single channel events revealed γ_j of the size range 40–100 pS. hMSC coupling via gap junctions to other cell types provides the basis for considering them as a therapeutic repair or cellular delivery system to syncytia such as the myocardium.

(Received 25 November 2003; accepted after revision 2 February 2004; first published online 6 February 2004)

Corresponding author I. S. Cohen: Department of Physiology and Biophysics, 8661 SUNY, Stony Brook, NY 11794-8661, USA. Email: icohen@physiology.pnb.sunysb.edu

Acute myocardial infarction (MI) afflicts millions of people each year inducing significant mortality and, in many of survivors, marked reductions in myocyte number and in cardiac pump function. Adult cardiac myocytes divide only rarely, and the usual response to myocyte cell loss is hypertrophy that often progresses to congestive heart failure, a disease with a high annual mortality. Great excitement has been generated by recent reports of the delivery of human mesenchymal stem cells (hMSCs; a multipotent cell population of blood lineage) to the hearts of post-MI patients resulting in improved mechanical performance (Strauer *et al.* 2002; Perin *et al.* 2003). Earlier studies using mice show that hMSCs found within the myocardium differentiate into a cardiomyocyte phenotype (Toma *et al.* 2002) and in the case of the pig, hMSCs can effect repair when coinjected with fetal pig cardiomyocytes

(Min *et al.* 2002). In the baboon, stem cells have been shown to stimulate angiogenesis (Norol *et al.* 2002). The presumption in these and other animal studies (Orlic *et al.* 2001) is that the hMSCs integrate into the cardiac syncytium. For any such cell to become an effective member of the myocardium it is necessary for the hMSCs and/or differentiating cell type to form gap junctions with the surrounding tissue. Indeed, recent studies using haematopoietic progenitor cells, a subpopulation of the marrow stem cell population, reveal Cx43-like gap junctions mediate intercellular communication (Durig *et al.* 2000). In this study we demonstrate that hMSC connexins, the building block proteins of gap junctions, can form functional gap junctions with one another, with cell lines expressing cardiac connexins, and with adult cardiac myocytes. Further, the connexins expressed suggest

that hMSCs should readily integrate into electrical syncytia of many tissues promoting repair or serving as the substrate for a therapeutic delivery system.

Methods

Cells and culture conditions

Human mesenchymal stem cells (hMSCs; mesenchymal stem cells, human bone marrow; Poietics™) were purchased from Clonetics/BioWhittaker (Walkersville, MD, USA) and cultured in mesenchymal stem cell (MCS) growth medium and used from passages 2–4. Isolated and purified hMSCs can be cultured for many passages (12) without losing their unique properties, i.e. normal karyotype and telomerase activity (van den Bos *et al.* 1997; Pittenger *et al.* 1999). HeLa cells that were transfected with rat Cx40, rat Cx43 or mouse Cx45 were cocultured with hMSCs. Production, characterization and culture conditions of transfected HeLa cells have been previously described (Valiunas *et al.* 2000, 2002). Adult dogs of either sex were killed by an approved protocol at SUNY Stony Brook by an injection of sodium pentobarbital (80 mg kg⁻¹ body weight). Cardiomyocytes were isolated from the canine ventricle as previously described (Yu *et al.* 2000). We have adopted the method of primary culture of canine cardiomyocytes following the procedure described for mouse cardiomyocytes (Zhou *et al.* 2000). The cardiomyocytes were plated at 0.5–1 (10⁴ cells cm⁻² in minimal essential medium (MEM) containing 2.5% fetal bovine serum (FBS) and 1% penicillin/streptomycin (PS) onto mouse laminin (10 µg ml⁻¹) precoated coverslips. After 1 h of culture in a 5% CO₂ incubator at 37°C, the medium was changed to FBS-free MEM. Stem cells were added after 24 h and coculture was maintained in Dulbecco's modified Eagle's medium (DMEM) with 5% FBS. Cell Tracker Green (Molecular Probes, Eugene, OR, USA) was used to distinguish hMSCs from HeLa cells in coculture in all experiments (Valiunas *et al.* 2000).

Anti-connexin antibodies, immunofluorescent labelling and immunoblot analysis of the cells

Commercially available mouse anticonnexin monoclonal and polyclonal antibodies (Chemicon International, Temecula, CA, USA) of Cx40, Cx43 and Cx45 were used for immunostaining and immunoblots as described earlier (Laing & Beyer, 1995). Fluorescein-conjugated goat antimouse or antirabbit IgG (ICN Biomedicals, Inc.) was used as secondary antibody.

Electrophysiological measurements

Glass coverslips with adherent cells were transferred to an experimental chamber perfused at room temperature (~22°C) with bath solution containing (mM): NaCl, 150; KCl, 10; CaCl₂, 2; Hepes, 5 (pH 7.4); glucose, 5. The patch pipettes were filled with solution containing (mM): potassium aspartate, 120; NaCl, 10; MgATP, 3; Hepes, 5 (pH 7.2); EGTA, 10 (pCa ~8); filtered through 0.22 µm pores. When filled, the resistance of the pipettes measured 1–2 MΩ. Experiments were carried out on cell pairs using a double voltage-clamp. This method permitted us to control the membrane potential (V_m) and measure the associated junctional currents (I_j).

Dye flux studies

Dye transfer through gap junction channels was investigated using cell pairs. Lucifer Yellow (LY) (Molecular Probes) was dissolved in the pipette solution to reach a concentration of 2 mM. Fluorescent dye cell-to-cell spread was imaged using a 16 bit 64 000 pixel grey scale digital CCD-camera (LYNXX 2000T, Spectra Source Instruments) (Valiunas *et al.* 2002). In experiments with heterologous pairs LY was always injected into the cells which were tagged with Cell Tracker Green. The injected cell fluorescence intensity derived from LY is 10–15 times higher than the initial fluorescence from Cell Tracker Green.

Signal recording and analysis

Voltage and current signals were recorded using patch clamp amplifiers (Axopatch 200). The current signals were digitized with a 16 bit A/D-converter (Digidata 1322A, Axon Instruments, Union City, CA, USA) and stored with a personal computer. Data acquisition and analysis were performed with pCLAMP 8 software (Axon Instruments). Curve fitting and statistical analyses were performed using SigmaPlot and SigmaStat, respectively (SPSS, Chicago, IL, USA). The results are presented as means ± s.e.m.

Results

The immunolocalization for Cx43 and Cx40 was seen along regions of intimate cell-to-cell contact and within regions of the cytoplasm of the hMSCs grown in culture as monolayers (Fig. 1A and B). Cx45 staining was also detected but unlike that of Cx43 or Cx40 was not typical of connexin distribution in cells. Rather it was characterized by fine granular cytoplasmic and reticular-like staining

with no readily observed membrane-associated plaques (Fig. 1C). This does not exclude the possibility that Cx45 channels exist but does imply that their number relative to Cx43 and Cx40 homotypic, heterotypic and heteromeric channels is low. Figure 1D illustrates Western blot analysis (Valiunas *et al.* 2001) for canine ventricle myocytes and hMSCs with a Cx43 polyclonal antibody which adds further proof of Cx43 presence in hMSCs.

Gap junctional coupling among hMSCs is demonstrated in Fig. 2. Junctional currents recorded between hMSC pairs show quasi-symmetrical (Fig. 2A) and asymmetrical (Fig. 2B) voltage dependency arising in response to symmetrical 10 s transjunctional voltage steps (V_j) of equal amplitude but opposite sign starting from ± 10 mV to ± 110 mV using increments of 20 mV. These behaviours are typically observed in cells which coexpress Cx43 and Cx40 (Valiunas *et al.* 2001).

Figure 2C summarizes the data obtained from hMSC pairs. The values of normalized instantaneous ($g_{j,inst}$, \circ) and steady state conductances ($g_{j,ss}$, \bullet) (determined at the

beginning and at the end of each V_j step, respectively) were plotted *versus* V_j . The left panel shows a quasi-symmetrical relationship from five hMSC pairs. The continuous curves represent the best fit of data to the Boltzmann equation with the following parameters: half-deactivation voltage, $V_{j,0} = -70/65$ mV; minimum g_j , $g_{j,min} = 0.29/0.34$; maximum g_j , $g_{j,max} = 0.99/1.00$; gating charge, $z = 2.2/2.3$ for negative/positive V_j , respectively. Summarized plots from six asymmetrical cases are shown in the right panel. The $g_{j,ss}$ declined in sigmoidal fashion at negative V_j and showed a reduced voltage sensitivity to positive V_j . Boltzman fitting for negative V_j revealed the following values: $V_{j,0} = -72$ mV, $g_{j,min} = 0.25$, $g_{j,max} = 0.99$, $z = 1.5$.

Figure 2D and E illustrates typical multichannel recordings from a hMSC pair. Using 120 mM potassium aspartate as a pipette solution we have observed channels with unitary conductances of 28–80 pS range. Operation of channels with ~ 50 pS conductance (see Fig. 2D) is consistent with previously published values (Valiunas

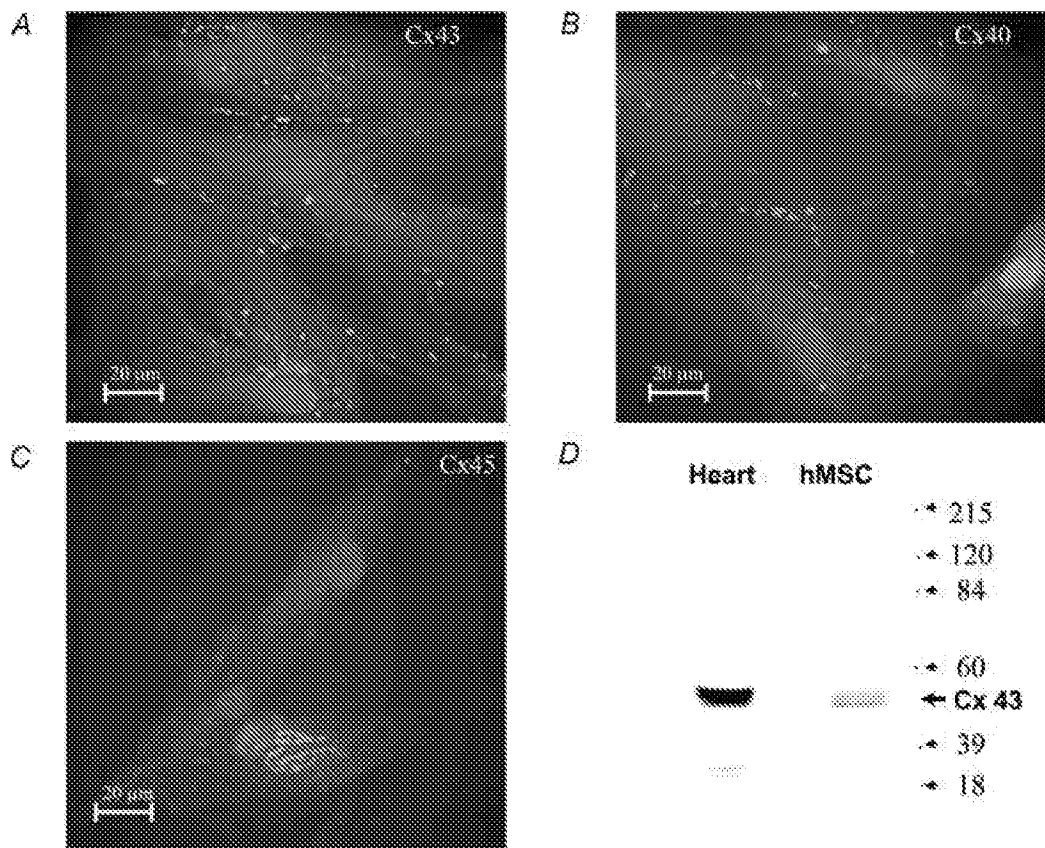


Figure 1. Identification of connexins in gap junctions of hMSCs

Immunostaining of Cx43 (A), Cx40 (B) and Cx45 (C). D, immunoblot analysis of Cx43 in canine ventricular myocytes and hMSCs. Whole cell lysates (120 μg) from ventricular cells or hMSCs were resolved by SDS, transferred to membranes, and blotted with Cx43 antibodies. Migration of molecular weight markers is indicated to the right of the blot.

et al. 1997, 2002) for Cx43 homotypic channels. This does not preclude the presence of other channel types; it merely suggests that Cx43 forms functional channels in hMSCs.

To further define the nature of the coupling we cocultured hMSCs with human HeLa cells stably transfected with Cx43, Cx40 and Cx45 (Elfgang *et al.* 1995) and found that hMSCs were able to couple to all these transfectants. Figure 3A illustrates an example of junctional currents recorded between hMSC and HeLaCx43 cell pairs, one that manifested symmetrical and one that exhibited asymmetrical voltage-dependent currents in response to a series (from ± 10 mV to ± 110 mV) of symmetrical transjunctional voltage steps (V_j). The quasi-symmetrical record suggests that the dominant functional channel is homotypic Cx43 while

the asymmetrical record suggests the activity of another connexin in the hMSC (presumably Cx40 as shown by immunohistochemistry, see Fig. 1) that could be either a heterotypic or heteromeric form or both. These records are similar to those previously published for transfected cells: heterotypic and mixed/heteromeric forms of Cx40 and Cx43 (Valiunas *et al.* 2000, 2001). Coculture of hMSCs with HeLa cells transfected with Cx40 (Fig. 3B) also revealed symmetrical and asymmetrical voltage-dependent junctional currents consistent with the coexpression of Cx43 and Cx40 in the hMSCs similar to the data for HeLaCx43–hMSC pairs. HeLa cells transfected with Cx45 that coupled to hMSCs always produced asymmetrical junctional currents with pronounced voltage gating when the Cx45 (HeLa) side was negative (Fig. 3C). This is consistent with the dominant

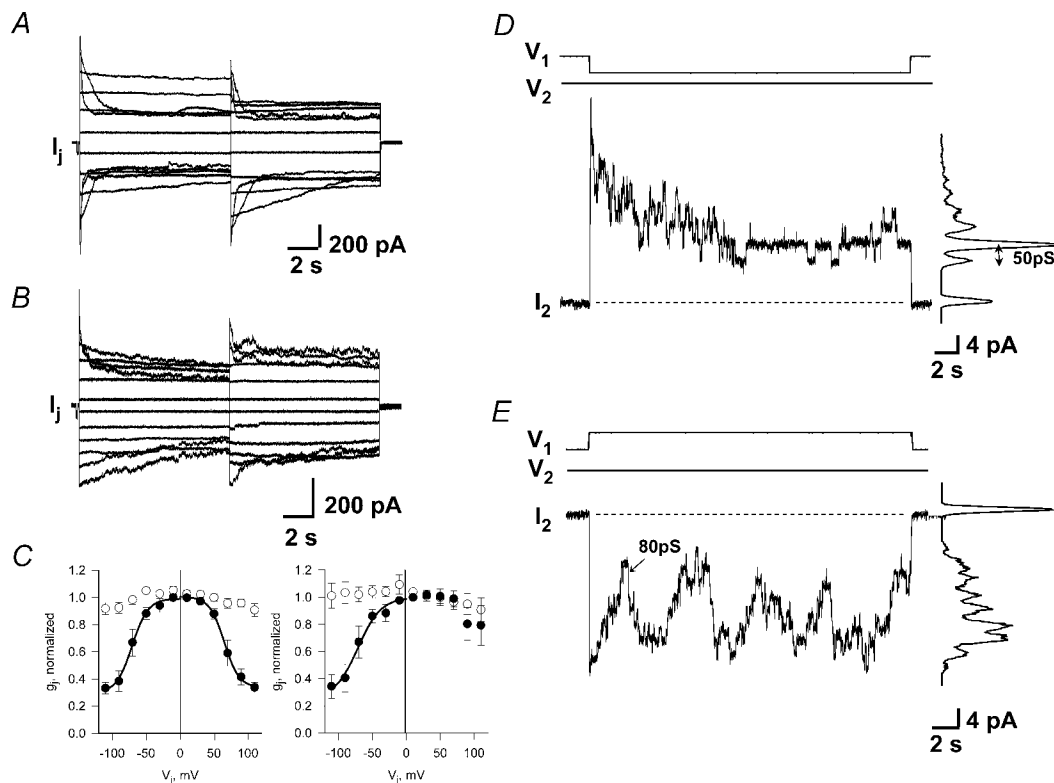


Figure 2. Macroscopic and single channel properties of gap junctions between hMSC pairs

Gap junction currents (I_j) elicited from hMSCs using a symmetrical bipolar pulse protocol (10 s, from ± 10 mV to ± 110 mV, $V_h = 0$ mV) showed two types of voltage-dependent current deactivation: symmetrical (A) and asymmetrical (B). C, summary plots of normalized instantaneous (○) and steady-state (●) g_j versus V_j . Left panel, quasi-symmetrical relationship from 5 pairs; continuous line, Boltzmann fit: $V_{j,0} = -70/65$ mV, $g_{j,min} = 0.29/0.34$, $g_{j,max} = 0.99/1.00$, $z = 2.2/2.3$ for negative/positive V_j . Right panel, asymmetrical relationship from 6 pairs; Boltzmann fit for negative V_j : $V_{j,0} = -72$ mV, $g_{j,min} = 0.25$, $g_{j,max} = 0.99$, $z = 1.5$. D and E, single channel recordings from pairs of hMSCs. Pulse protocol (V_1 and V_2) and associated multichannel currents (I_2) recorded from a cell pair during maintained V_j of ± 80 mV. The discrete current steps indicate the opening and closing of single channels. Dashed line: zero current level. The all points current histograms on the right-hand side reveal a conductance of ~ 50 pS.

channel forms in the hMSC being Cx43 and Cx40 as both produce asymmetrical currents when they form heterotypic channels with Cx45 (Valiunas *et al.* 2000, 2001). This does not exclude Cx45 as a functioning channel in hMSCs but it does indicate that Cx45 is a minor contributor to cell to cell coupling in hMSCs. The lack of

visualized plaques in the immunostaining for Cx45 (Fig. 1) further supports this interpretation.

The summarized plots of $g_{j,ss}$ versus V_j from pairs between hMSC and transfected HeLa cells are shown in Fig. 3D. The left panel shows the results from hMSC–HeLaCx43 pairs. For symmetrical data (●, four

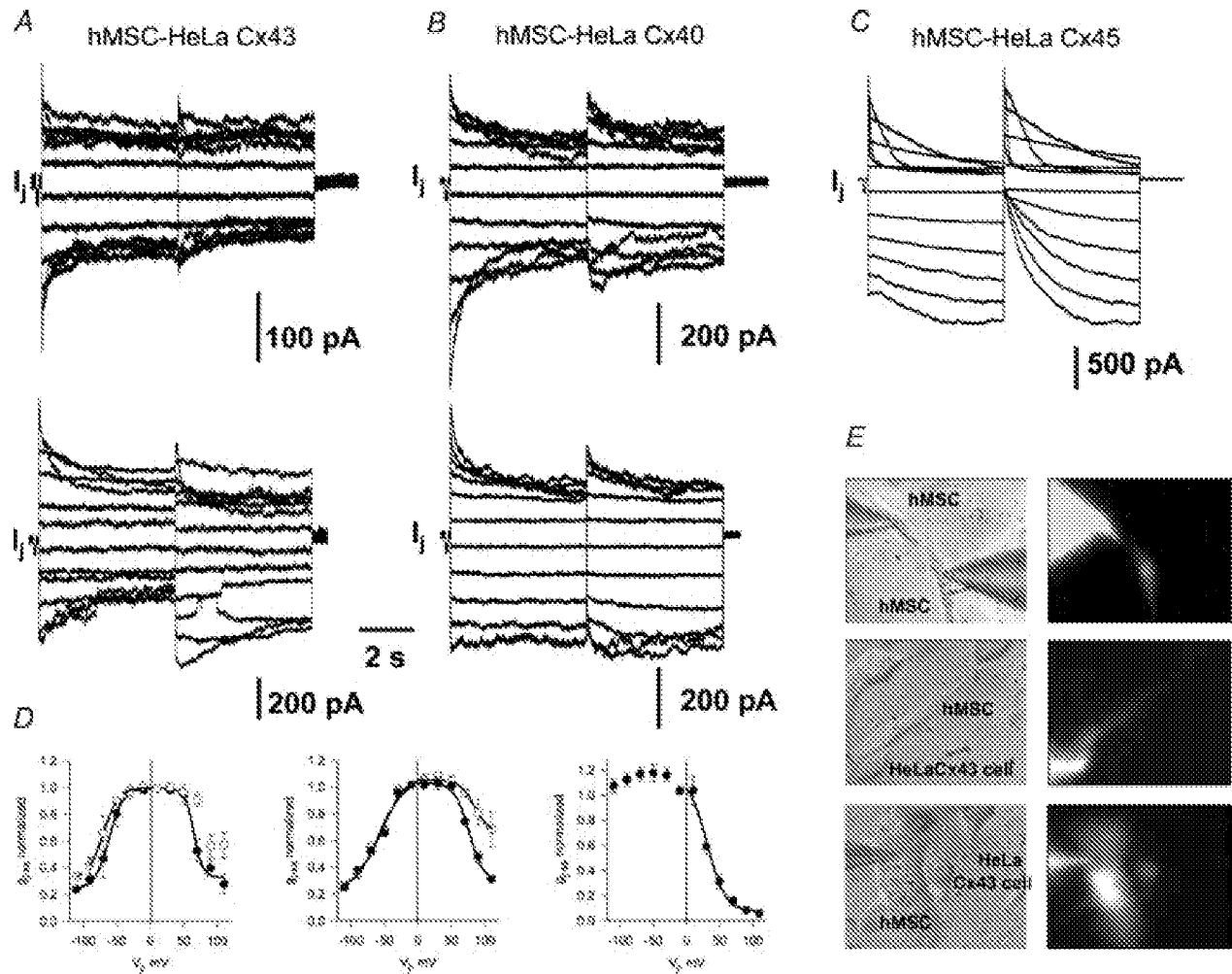


Figure 3. Macroscopic junctional currents in cell pairs between a hMSC and HeLa cell expressing only Cx40, Cx43 or Cx45

In all cases hMSC to HeLa cell coupling was tested 6–12 h after initiating coculture. *A*, I_j elicited in response to a series of 5 s voltage steps (V_j) in hMSC–HeLaCx43 pairs. Top, symmetrical current deactivation; bottom, asymmetrical current–voltage dependence. *B*, macroscopic I_j recordings from hMSC–HeLaCx40 pairs exhibit symmetrical (top panel) and asymmetrical (bottom panel) voltage-dependent deactivation. *C*, asymmetrical I_j from an hMSC–HeLaCx45 pair exhibits voltage-dependent gating when the Cx45 side is relative negative. I_j recorded from hMSC. *D*, $g_{j,ss}$ plots versus V_j from pairs between hMSC and transfected HeLa cells. Left panel, hMSC–HeLaCx43 pairs, quasi-symmetrical relationship (●) and asymmetrical relationship (○); continuous and dashed lines are Boltzmann fits (see text for details). Middle panel, symmetrical (●) and asymmetrical (○) relationships from hMSC–HeLaCx40 pairs; the continuous and dashed lines correspond to Boltzmann fits (see text for details). Right panel, asymmetrical relationship from hMSC–HeLaCx45 cell pairs; continuous line, Boltzmann fit for positive V_j (see text for details). *E*, cell-to-cell Lucifer Yellow (LY) spread in cell pairs: from an hMSC to an hMSC (upper panel), from a HeLaCx43 to an hMSC (middle panel) and from an hMSC to a HeLaCx43 (bottom panel). In all cases a pipette containing 2 mM LY was attached to the left-hand cell in the whole-cell configuration. Epifluorescent micrographs taken at 12 min after dye injection show LY spread to the adjacent (right-hand) cell. The simultaneously measured junctional conductance revealed g_j of ~13 nS, ~16 nS and ~18 nS of the pairs, respectively.

preparations), Boltzmann fits (continuous lines) yielded the following parameters: $V_{j,0} = -61/65$ mV, $g_{j,\min} = 0.24/0.33$, $g_{j,\max} = 0.99/0.99$, $z = 2.4/3.8$ for negative/positive V_j . For asymmetrical data (\circ , three preparations), the Boltzmann fit (dashed line) at negative V_j values revealed the following parameter values: $V_{j,0} = -70$ mV, $g_{j,\min} = 0.31$, $g_{j,\max} = 1.00$, $z = 2.2$. The middle panel shows data from hMSC–HeLaCx40 pairs including three symmetrical (\bullet) and two asymmetrical (\circ) $g_{j,ss}$ – V_j relationships. The continuous lines correspond to a Boltzmann fit to symmetrical data ($V_{j,0} = -57/76$ mV, $g_{j,\min} = 0.22/0.29$, $g_{j,\max} = 1.1/1.0$, $z = 1.4/2.3$; negative/positive V_j) and the dashed line is a fit to the asymmetrical data ($V_{j,0} = -57/85$ mV, $g_{j,\min} = 0.22/0.65$, $g_{j,\max} = 1.1/1.0$, $z = 1.3/2.2$; negative/positive V_j). The data from the six complete experiments from hMSC–HeLaCx45 cell pairs are shown on the right panel. The $g_{j,ss}$ plot *versus* V_j was strongly asymmetrical and the best fit of the data to the Boltzmann equation at positive V_j values revealed following parameter values: $V_{j,0} = 31$ mV, $g_{j,\min} = 0.07$, $g_{j,\max} = 1.2$, $z = 1.8$.

Figure 3E shows Lucifer Yellow transfer from an hMSC to an hMSC (upper panel), from a HeLaCx43 to an hMSC (middle panel) and from an hMSC to a HeLaCx43 (bottom panel). The junctional conductance of the cell pairs was simultaneously measured by methods described earlier (Valiunas *et al.* 2002) and revealed conductances of ~ 13 , ~ 16 and ~ 18 nS, respectively. The transfer of Lucifer Yellow was similar to that previously reported for homotypic Cx43 or coexpressed Cx43 and Cx40 in HeLa cells (Valiunas *et al.* 2002). Cell Tracker Green was always used in one of the two populations of cells to allow heterologous pairs to be identified (Valiunas *et al.* 2000). Lucifer Yellow was always delivered to the cell containing cell tracker. The fluorescence intensity generated by the Cell Tracker Green was 10–15 times less than fluorescence intensity produced by the concentration of Lucifer Yellow delivered to the source cell.

We also cocultured hMSCs with adult canine ventricular myocytes as shown in Fig. 4. Immunostaining for Cx43 was detected between the rod-shaped ventricular myocytes and hMSCs as shown in Fig. 4A. The hMSCs also couple electrically with cardiac myocytes. Both macroscopic (Fig. 4B) and multichannel (Fig. 4C) records were obtained. Junctional currents in Fig. 4B are asymmetrical while those in Fig. 4C show unitary events of the size range typically resulting from the operation of homotypic Cx43 or heterotypic Cx43–Cx40 or homotypic Cx40 channels (Valiunas *et al.* 2000, 2001). Heteromeric forms are also possible whose conductances are the same or similar to homotypic or heterotypic forms.

In studies of cell pairs we have demonstrated effective coupling of hMSC to other hMSC (total gap junction conductance 13.8 ± 2.4 nS, $n = 14$), to HeLaCx43 (7.9 ± 2.1 nS, $n = 7$), to HeLaCx40 (4.6 ± 2.6 nS, $n = 5$), to HeLaCx45 (11 ± 2.6 nS, $n = 6$) and to ventricular myocyte (1.5 ± 1.3 nS, $n = 4$).

Discussion

Our results show that hMSCs couple to one another via Cx43 and Cx40. In addition, they form functional gap junction channels with cells transfected with Cx43, Cx40 or Cx45 as well as canine ventricular cardiomyocytes.

What are the implications of junctional current asymmetry recorded from various cell pairs including an hMSC? A number of studies have shown that heterotypic gap junction channels typically generate asymmetrical currents while heteromeric mixtures give rise to symmetrical-like (weakly asymmetrical) currents. Co-expression of two connexins is expected to display variability in terms of symmetry and asymmetry based on the population size of homotypic, heterotypic and potential heteromeric channel forms. The size of the homotypic, heterotypic and heteromeric populations would be dependent on connexin–connexin interactions during assembly and connexon–connexon interactions in the plasma membranes of two closely apposed cells (Brink *et al.* 1997; Valiunas *et al.* 2001; Beyer & Berthoud, 2002). In the case of the stem cell pairs, assuming only Cx43 and Cx40 are coexpressed, only two types of heterotypic channels are possible, each with equal but oppositely signed voltage dependence. Two equally distributed populations will result in symmetrical behaviour while unequal distribution (dominance of one form over the other) will result in asymmetry. This is consistent with the data and interpretation of Valiunas *et al.* (2000, 2001). Any number of possible heteromeric forms are also potential candidates for generating asymmetrical junctional currents. The problem is that no one single form (of 192 possible for two coexpressing connexins) can be studied in isolation from others. Thus attributing asymmetry to heteromeric forms is equivocal. If all the connexins had equal affinity for each other and themselves then coexpression of two connexins would be dominated by heteromeric forms. If on the other hand self-recognition and affinity are preferred over heterologous interactions then homotypic forms would dominate.

Lucifer Yellow passage between an hMSC and HeLaCx43 cell (see Fig. 3F) is yet another indicator of robust gap junction-mediated coupling. The transfer of Lucifer Yellow between hMSCs and HeLa cells transfected with Cx43

is similar to that of homotypic Cx43 or coexpressed Cx43 and Cx40. It excludes homotypic Cx40 as a dominating channel type as Cx40 is some 5 times less permeable to Lucifer Yellow than Cx43 (Valiunas *et al.* 2002).

We have defined the lower limit or minimum number of functional connexins present in stem cells (Cx43, Cx40 and possibly Cx45). The literature has already provided us with examples of hMSC transformation into heart cells (Toma

et al. 2002). Does the functional expression of connexins change under such transformations and as a consequence affect coupling, or are hMSCs fixed with regard to the pool of potentially expressible connexins? This is yet to be determined. Our results show that hMSCs couple to one another via Cx43 and Cx40. We have also established that hMSCs can form heterologous junctions with cardiac myocytes and cultured HeLa cells transfected with specific connexins (Cx40, Cx43, Cx45).

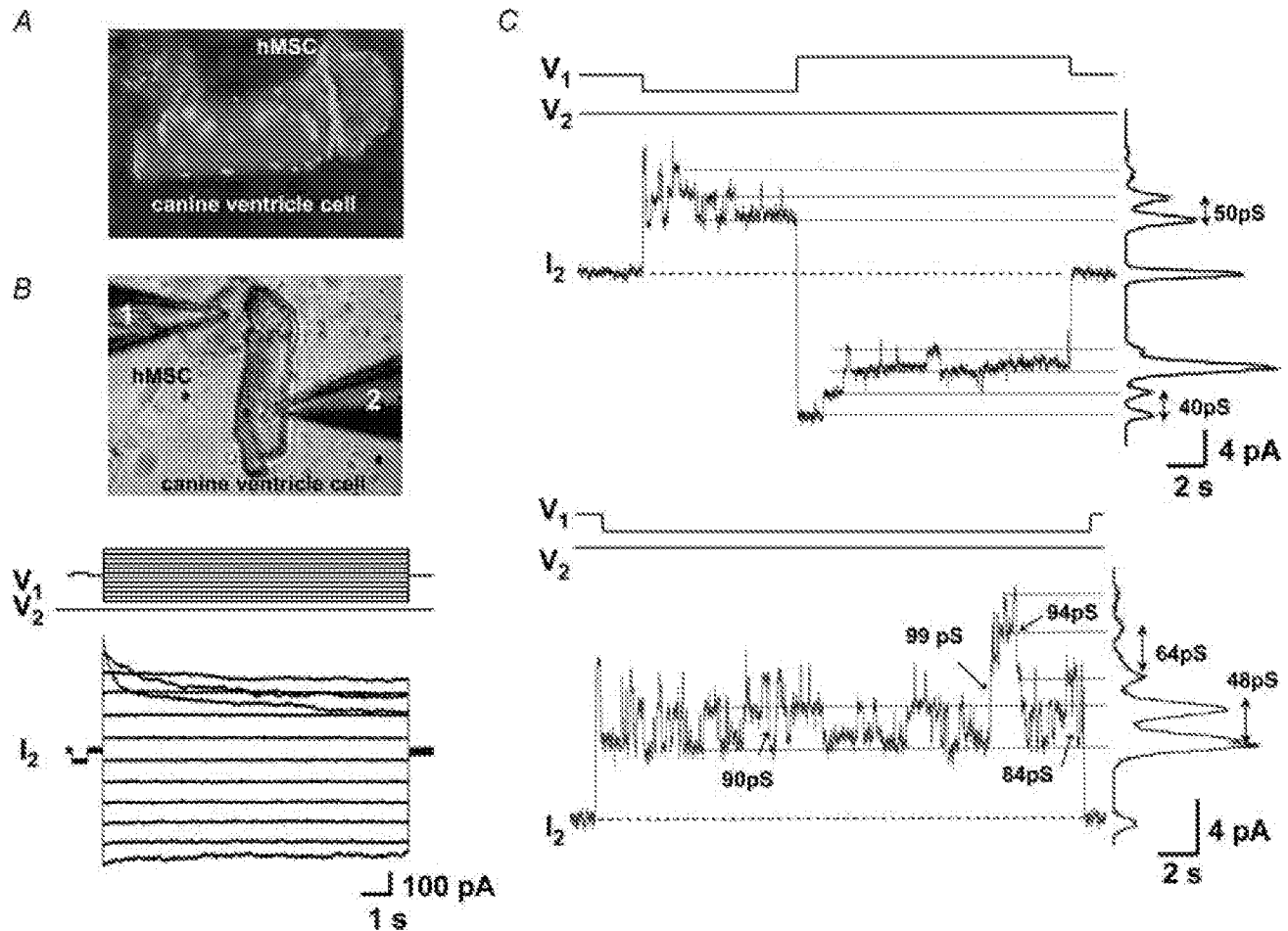


Figure 4. Macroscopic and single channel properties of gap junctions between hMSC-canine ventricle cell pairs

Myocytes were plated between 12 and 72 h and cocultured with hMSCs for 6–12 h before measuring coupling. *A*, localization of Cx43 for hMSC-canine ventricle cell pairs. Most of Cx43 was localized to the ventricular cell ends and a small amount of Cx43 was present along the lateral borders. The intensive Cx43 staining was detected between the end of the rod-shaped ventricular cell (middle cell) and the hMSC (right cell). There is no detectable Cx43 staining between the ventricular cell and the hMSC on the left side. *B*, top, phase-contrast micrograph of a hMSC-canine ventricular myocyte pair. Bottom, monopolar pulse protocol (V_1 and V_2) and associated macroscopic junctional currents (I_2) exhibiting asymmetrical voltage dependence. *C*, top, multichannel current elicited by symmetrical biphasic 60 mV pulse. Dashed line, zero current level; dotted lines, represent discrete current steps indicative of opening and closing of channels. The current histograms yielded a conductance of ~ 40 – 50 pS. Bottom, multichannel recording during maintained V_j of 60 mV. The current histograms revealed several conductances of 48–64 pS with several events with conductance of 84 pS to 99 pS (arrows) which resemble operation of Cx43, heterotypic Cx40–Cx43 and/or homotypic Cx40 channels.

To date, there are more than 20 connexins identified in humans encoded by a multigene family (Beyer & Berthoud, 2002). We recognize that there is the potential for the expression of other connexins in hMSCs. However, our present study focused on cardiac-specific connexins. Our data strongly suggest that Cx43 and Cx40 are dominant functional forms in stem cells. We have also probed for Cx26 and Cx32 and found no expression (data not shown). A thorough demonstration of which connexins are expressed of the many human connexins awaits further investigation.

The hMSC–cardiomyocyte coupling conductance was notably lower than those values obtained from hMSC–HeLa cell pairs. The gap junction conductance between hMSC–cardiomyocyte pairs ranged from 0.1 to 5.5 nS, which reflects an approximate range of 2–110 channels and is considerably lower compared to conductance values (40–200 nS) reported earlier for adult ventricular cell pairs (Maurer & Weingart, 1987; Polontchouk *et al.* 2002). The lower value might, in fact, reflect a reduced ability of hMSCs and cardiomyocytes to form gap junctions, which could be influenced by several experimental conditions and factors. The first is the amount of time given for the hMSC to form junctions with the cardiomyocytes, which typically was less than 12 h. After that time the hMSCs become flattened and spread out, making contacts with many other hMSCs. To find a single hMSC–cardiomyocyte pair then is rather difficult. Second, in the freshly isolated cardiomyocytes, Cx43 immunolocalizes mostly at intercalated discs at the cell ends (Huang *et al.* 1996; Eppenberger & Zuppinger, 1999) (see also Fig. 4A). Therefore, the lower junctional conductance between hMSCs and myocytes is to some degree configuration dependent where the hMSC must contact the end of a myocyte. This latter conformation, illustrated in Fig. 4A, was not common. Finally, the reduction in gap junction expression over the first 48 h after isolation and subsequent culturing (Huang *et al.* 1996) plays a significant role. It is entirely possible that prolonged coculturing of hMSCs with cardiomyocytes would reveal heterogeneous cell pairs with larger junctional conductances than reported here but the technical reasons cited above limit our ability to define the meaning of the low junctional conductance measured between hMSCs and myocytes. Moreover, it has been found that the formation of only ~15 channels and possibly even less is quite sufficient to ensure action potential propagation in neonatal rat heart cells (Rook *et al.* 1988, 1990). In a preliminary report we have shown that these same hMSCs transfected with a pacemaker gene (HCN2) are able to effect alterations in pacing *in situ* and *in vitro*, which strongly suggests that the level of coupling

between hMSCs and myocytes is physiologically sufficient (Plotnikov *et al.* 2003).

Related studies have shown that skeletal muscle myotubes can effect some measure of cardiac repair but a recent study by Leobon *et al.* (2003) has shown *in vitro* that myotubes do not form gap junctions with cardiac myocytes. While the data of that study exclude gap junction-mediated communication (*in vitro*) it does not eliminate other forms of interaction between cells. One possibility is ephaptic-like transmission similar to the work of Arvantitaki and collaborators that is referred to by Eccles (1964). Other characterizations of electrical transmission without gap junctions are summarized by Bennett (1977). The experimental procedures used by Leobon *et al.* (2003) would not define or illustrate a 'restricted space' electrical synapse like those examples given by Bennett (1977). A further complication in interpreting the data of Leobon *et al.* (2003) is the fact that their experiments are done *in vitro* with cardiac myocytes and the cited data illustrating myotubes enhanced performance is *in situ*. The myotubes *in situ* might well have differentiated and possibly formed junctions with cardiac myocytes.

These data support the possibility of using hMSCs as a therapeutic substrate for repair of cardiac tissue. Other syncytia such as vascular smooth muscle or endothelial cells should also be able to couple to the hMSCs because of the ubiquity of Cx43 and Cx40 (Wang *et al.* 2001). Thus they might also be amenable to hMSC-based therapeutics, as follows: hMSCs can be transfected to express ion channels which then can influence the surrounding syncytial tissue. Alternatively, the hMSCs can be transfected to express genes that produce small therapeutic molecules capable of permeating gap junctions and influencing recipient cells. Further, for short-term therapy, small molecules can be directly loaded into hMSCs for delivery to recipient cells. The success of such an approach is critically dependent on gap junction channels as the final conduit for delivery of the therapeutic agent to the recipient cells. We have demonstrated the feasibility of one such approach by transfecting hMSCs with mHCN2, a gene encoding the cardiac pacemaker channel, and delivering them to the canine heart where they generate a spontaneous rhythm (Plotnikov *et al.* 2003).

References

- Bennett MVL (1977). Electric transmission: a functional analysis and comparison to chemical transmission. In *Handbook of Physiology*, section 1 *The Nervous System*, vol. I, *Cellular Biology of Neurons*, ed. Brookhart JM, Mountcastle VB, Kandel ER & Geiger SR, pp. 357–416. American Physiological Society, Bethesda, MD, USA.

- Beyer EC & Berthoud VM (2002). Gap junction synthesis and degradation as therapeutic targets. *Curr Drug Targets* **3**, 409–416.
- Brink PR, Cronin K, Banach K, Peterson E, Westphale EM, Seul KH, Ramanan SV & Beyer EC (1997). Evidence for heteromeric gap junction channels formed from rat connexin43 and human connexin37. *Am J Physiol* **273**, C1386–C1396.
- Durig J, Rosenthal C, Halfmeyer K, Wiemann M, Novotny J, Bingmann D, Duhrsen U & Schirmmacher K (2000). Intercellular communication between bone marrow stromal cells and CD34+ haematopoietic progenitor cells is mediated by connexin 43-type gap junctions. *Br J Haematol* **111**, 416–425.
- Eccles JC (1964). *The Physiology of Synapses*, p. 145. Academic Press Inc, New York.
- Elfgang C, Eckert R, Lichtenberg-Frate H, Butterweck A, Traub O, Klein RA, Hulser DF & Willecke K (1995). Specific permeability and selective formation of gap junction channels in connexin-transfected HeLa cells. *J Cell Biol* **129**, 805–817.
- Eppenberger HM & Zuppinger C (1999). In vitro reestablishment of cell-cell contacts in adult rat cardiomyocytes. Functional role of transmembrane components in the formation of new intercalated disk-like cell contacts. *FASEB J* **13** (suppl.), S83–S89.
- Huang XD, Horackova M & Pressler ML (1996). Changes in the expression and distribution of connexin 43 in isolated cultured adult guinea pig cardiomyocytes. *Exp Cell Res* **228**, 254–261.
- Laing JG & Beyer EC (1995). The gap junction protein connexin43 is degraded via the ubiquitin proteasome pathway. *J Biol Chem* **270**, 26399–26403.
- Leobon B, Garcin I, Menasche P, Vilquin JT, Audinat E & Charpak S (2003). Myoblasts transplanted into rat infarcted myocardium are functionally isolated from their host. *Proc Natl Acad Sci U S A* **100**, 7808–7811.
- Maurer P & Weingart R (1987). Cell pairs isolated from adult guinea pig and rat hearts: effects of $[Ca^{2+}]_i$ on nexal membrane resistance. *Pflügers Arch* **409**, 394–402.
- Min JY, Sullivan MF, Yang Y, Zhang JP, Converso KL, Morgan JP & Xiao YF (2002). Significant improvement of heart function by cotransplantation of human mesenchymal stem cells and fetal cardiomyocytes in postinfarcted pigs. *Ann Thorac Surg* **74**, 1568–1575.
- Norol F, Merlet P, Isnard R, Bonnet N, Sebillion P, Ribeiro M, Pradeau P, Vernant JP & Herodin F (2002). Evaluation of myocardial infarct repair by mobilized stem cells in a primate model. *Blood* **100**, 93.
- Orlic D, Kajstura J, Chimenti S, Jakoniuk I, Anderson SM, Li B, Pickel J, McKay R, Nadal-Ginard B, Bodine DM, Leri A & Anversa P (2001). Bone marrow cells regenerate infarcted myocardium. *Nature* **410**, 701–705.
- Perin EC, Geng YJ & Willerson JT (2003). Adult stem cell therapy in perspective. *Circulation* **107**, 935–938.
- Pittenger MF, Mackay AM, Beck SC, Jaiswal RK, Douglas R, Mosca JD, Moorman MA, Simonetti DW, Craig S & Marshak DR (1999). Multilineage potential of adult human mesenchymal stem cells. *Science* **284**, 143–147.
- Plotnikov AN, Shlapakova IN, Danilo P, Herron A, Potapova I, Lu Z, Valiunas V, Doronin S, Brink PR, Robinson RB, Cohen IS & Rosen MR (2003). Human mesenchymal stem cells transfected with HCN2 as a gene delivery system to induce pacemaker function in canine heart. *Circulation* **108**, IV-547.
- Polontchouk LO, Valiunas V, Haeffliger JA, Eppenberger HM & Weingart R (2002). Expression and regulation of connexins in cultured ventricular myocytes isolated from adult rat hearts. *Pflügers Arch* **443**, 676–689.
- Rook MB, de Jonge B, Jongsma HJ & Masson-Pevet MA (1990). Gap junction formation and functional interaction between neonatal rat cardiocytes in culture: a correlative physiological and ultrastructural study. *J Membr Biol* **118**, 179–192.
- Rook MB, Jongsma HJ & van Ginneken AC (1988). Properties of single gap junctional channels between isolated neonatal rat heart cells. *Am J Physiol* **255**, H770–H782.
- Strauer BE, Brehm M, Zeus T, Kosterling M, Hernandez A, Sorg RV, Kogler G & Wernet P (2002). Repair of infarcted myocardium by autologous intracoronary mononuclear bone marrow cell transplantation in humans. *Circulation* **106**, 1913–1918.
- Toma C, Pittenger MF, Cahill KS, Byrne BJ & Kessler PD (2002). Human mesenchymal stem cells differentiate to a cardiomyocyte phenotype in the adult murine heart. *Circulation* **105**, 93–98.
- Valiunas V, Beyer EC & Brink PR (2002). Cardiac gap junction channels show quantitative differences in selectivity. *Circ Res* **91**, 104–111.
- Valiunas V, Bukauskas FF & Weingart R (1997). Conductances and selective permeability of connexin43 gap junction channels examined in neonatal rat heart cells. *Circ Res* **80**, 708–719.
- Valiunas V, Gemel J, Brink PR & Beyer EC (2001). Gap junction channels formed by coexpressed connexin40 and connexin43. *Am J Physiol Heart Circ Physiol* **281**, H1675–H1689.
- Valiunas V, Weingart R & Brink PR (2000). Formation of heterotypic gap junction channels by connexins 40 and 43. *Circ Res* **86**, E42–E49.
- van den Bos C, Mosca JD, Winkles J, Kerrigan L, Burgess WH & Marshak DR (1997). Human mesenchymal stem cells respond to fibroblast growth factors. *Hum Cell* **10**, 45–50.
- Wang HZ, Day N, Valcic M, Hsieh K, Serels S, Brink PR & Christ GJ (2001). Intercellular communication in cultured human vascular smooth muscle cells. *Am J Physiol Cell Physiol* **281**, C75–C88.
- Yu H, Gao J, Wang H, Wymore R, Steinberg S, McKinnon D, Rosen MR & Cohen IS (2000). Effects of the renin-angiotensin system on the current $I_{(to)}$ in epicardial and endocardial ventricular myocytes from the canine heart. *Circ Res* **86**, 1062–1068.

Zhou YY, Wang SQ, Zhu WZ, Chruscinski A, Kobilka BK, Ziman B, Wang S, Lakatta EG, Cheng H & Xiao RP (2000). Culture and adenoviral infection of adult mouse cardiac myocytes: methods for cellular genetic physiology. *Am J Physiol Heart Circ Physiol* **279**, H429–H436.

Acknowledgements

The authors acknowledge the technical assistance of S. Gaynullina and C. Metteewie. This work was supported by National Institute of Health and American Heart Association grants HL28958, HL20558, HL67101, GM55263, AHA0335236N, EY14604 and DK60037.